2019年度

筑波大学情報学群情報科学類

卒業研究論文

題目

Analysis of Sports Movements Based on Time-Series Pose Data (時系列姿勢データに基づくスポーツ動作の解析)

主専攻　ソフトウェアサイエンス主専攻

著者　スコット アトム

指導教員　福井 和広

Abstract

-

Contents

List of Figures

List of Tables

Chapter 1

Introduction

1.1 Overview

A long standing goal in the field of classification is to develop effective techniques which are applicable to real life problems. With recent advancements in motion tracking technology, significant strides towards this goal has been made due to the increased ability to capture richer and more fine-grained human motion data. In parallel, exponential growth in computer processing power has led to an incredible improvement in machine learning methods. For example there have been multiple breakthroughs in object detection, voice recognition and language modeling etc. However, despite this progress, there are relatively few studies which effectively couple the advancements of these technologies to human motion analysis. There are a wide range of benefits can be received by progressing research in human motion analysis. One example we find could significantly benefit is the prevention of injury in sport. For professional athletes, sustaining an injury directly leads to an economic loss. For elite young athletes an injury has the potential to squander hopes and dreams of playing as a professional. For societies with healthcare, an injury for an can represent a significant economic cost to society, with studies showing the mean medical cost of a high school varsity athlete was $709 per injury, $2223 per injury in human capital costs, and $10432 per injury in comprehensive costs [?].

Although there are many studies on the topic of injury prevention, these usually are from either a rigorously medical perspective [?] or a analysis made with a focus on machine learning with empirical (big) data [?]. This is a sizeable gap in which we try to bridge.

In this study, we aim to find factors that differentiate the motion between athletes who are at risk of injury. In order to do so, we develop models and techniques that allow us to analyse granular motion data of a well studied sensori-motor control task, the single-leg drop jump (SDJ).

We demonstrate that the methods introduced can be used to to detect anomalous motions. Moreover, we show that by interpreting the decision mechanism that led to the results can provide valuable practical information.

1.2 Contributions

In summary our research makes the following contributions,

1. A Method to prevent injuries with computer vision and machine learning Explanation.
2. A framework that returns actionable intelligence as feedback that can be utilised to improve the subjects movement
3. Novel research that intersects injury prevention, motion capture and machine learning.

1.3 Structure

The structure of this thesis is as follows; In chapter 2 we explain previous research on injury mechanisms in sport and methods for re

Chapter 2

Sensorimotor Performance Indicators

"Sensorimotor" indicates the involvement of both sensory and motor functions. The ability to execute sensorimotor tasks well is crucial for performance in athletic activity. Moreover, there is an abundance of research suggesting the connection between sensorimotor performance and injury. Therefore, great effort is directed to understanding these skills. In this section we will briefly review the literature intersecting sensorimotor performance and injury. In particular we will also introduce a method that involves an action known as the single leg drop jump (SLDJ) which is frequently used to measure sensorimotor performance.

2.0.1 Single-Leg Drop Jump

SLDJ is a unilateral horizontal drop jump, in other words the subject hops off an elevated platform of usually 30cms. It has shown to be more reliable, in means of reproducibility, than other sensorimotor performance tasks and is known to show similarities to the bilateral drop jump which is used is many areas including athlete assessment, performance monitoring, talent identification and rehabilitation [1].

There are largely two methods of measuring a SLDJ. The first is by measuring the ground reactions forces (GRFs) using a special measurement device known as a force plate. Several indicators such as Time to stabilization (TTS) [2], dynamic postural stability index (DPSI) [3] center of pressure (COP) [2] are then calculated and are assessed. It is important to note that there are multiple variations to calculate the above methods due to the possibility of different sample rate, filter settings or trial length. Such variances can cause a difference on outcome values and are may lead to contradictory results [4].

A number of studies show that TTS, DPSI, COP can be used to differente participants between chronic ankle instability (CAI), functional ankle instability (FAI), anterior cruciate ligament etc [5]. Yet, to date, the interrelations among TTS, DPSI, and other indicators are largely unknown [3].

The second method of measurement of SDJ is the measurement of pose characteristics using either manual notation or automated motion capture. Captured data is then analysed manually. It has been shown that women have a greater valgus knee angle at time of initial contact then men performing a SLDJ [6]. However, due to the high-dimensional and multivariate nature of this data, there only a handful of research focusing on the

measurement of pose characteristics.

Chapter 3

Subspace Based Classification

Subspace analysis is a term used to describe a general framework used in computer vision, that is used for the comparison and classification of subspaces. In this section, we introduce typical approaches in subspace analysis, in particular the classification of subspaces, and describe how it can be extended to analyse shapes such as human poses.

3.1 Subspace Method

The Subspace method assumes an input vector x and k-class subspaces. Each class subspace approximates a data distribution for a single class. This approximation is obtained by applying Principle Component Analysis (PCA) to each class.
The similarity S of the input vector x to the i^{th} class subspace $\mathcal{Y}$ is defined based on either:

- The length of the projection of x to $\mathcal{Y}$ [7].
- The minimum angle between x and $\mathcal{Y}$ [8].

The length of an input vector x is often normalized to 1.0. In this case these two criteria are identical.
Since they are the same, from here on we think of the angle-based similarity S defined by the following equation:

$$S = \cos^2\theta = \sum_{i=1}^{k} \frac{(\mathrm{x}^\top \cdot \Phi_i)^2}{||\mathrm{x2}||^2}$$

Φ_i is the i^{th} orthogonal normal basis vector of the class subspace $\mathcal{Y}$, which are obtained from applying the PCA to a set of patterns of the class. In more rigorous terms, these orthonormal basis vectors can be obtained as the eigenvectors of the correlation matrix

$$\sum_{i=1}^{l} \mathrm{x}^{(i)}\mathrm{x}^{(i)\top} \quad where\ \mathrm{x}^{(i)} \in \mathbb{X}$$

of the class ($\mathbb{X}$ is the training dataset).

Learning Phase

1. Generate k class subspaces from each class by using PCA.

Recognition Phase

1. Calculate S between x and each subspace Q_i.
2. Classify the x into the class where S was calculated to be the highest.

3.2 Mutual Subspace Method

The Mutual Subspace Method (MSM) is an extension of the Subspace Method (SM), where instead of having an input vector x, we use an input subspace $\mathscr{P}$. MSM is commonly used for image set classification [9].
The Subspace method assumes an input subspace and k class subspaces. Let us define the input subspace to be a d_p-dimensional subspace $\mathscr{P}$ and the class subspaces to be d_q-dimensional subspaces $\{\mathscr{Q}, \mathscr{R}, \mathscr{S}...\}$.
The similarity S between, for example, $\mathscr{P}$ and $\mathscr{Q}$ was originally defined as the minimum canonical angle θ_1. Canonical angles [?] are uniquely defined as:

$$\cos^2 \theta_i = \max_{\substack{u_i \perp u_j (=1,\ldots,i-1) \\ v_i \perp v_j (=1,\ldots,i-1)}} \frac{|(u_1, v_i)|^2}{||u_i||^2 ||v_i||^2}$$

Where $\mathrm{u}_i \in \mathscr{P}$, $\mathrm{v}_i \in \mathscr{Q}$, $||\mathrm{u}_i|| \neq 0$, $||\mathrm{v}_i|| \neq 0$.
We can also include the remaining canonical angles when calculating the similarity.

$$\tilde{S} = \frac{1}{t} \sum_{i=1}^{t} \cos \theta_i{}^2$$

This value $\tilde{S}$ reflects the structural similarity between two subspaces. It is also defined on the t smallest canonical angles. For practical applications, the canonical angles between subspaces $\mathcal{Y}_1$ and $\mathcal{Y}_2$ are obtained by calculating the singular values $\{\lambda_j\}_{j=1}^{m}$ of the correlation matrix between their basis matrices $\boldsymbol{Y}_1, \boldsymbol{Y}_2 \in \mathbb{R}^{d \times m}$, i.e. solving the SVD of $\boldsymbol{V} \boldsymbol{\Lambda} \boldsymbol{V}^\top = \boldsymbol{Y}_1{}^\top \boldsymbol{Y}_2$. This corresponds to finding the rotation of each basis that is closest to the opposing subspace. From solving this problem, the canonical angles can be obtained by $\theta_j = \cos^{-1}(\lambda_j)$, where $j = 1, \ldots, m$.
Learning Phase

1. Generate :math:‘k‘ class subspaces from each class by using PCA.

Recognition Phase

1. Calculate :math:‘S‘ (or :math:“) between :math:‘P‘ and each subspace :math:‘Q‘.
2. Classify :math:‘P‘ into the class where :math:‘S‘ (or :math:“) was calculated to be the highest.

3.2.1 Shape Subspace

3.2.2 Linear Discriminant Analysis

3.2.3 Canonical Angles

After generating a shape subspace from a single frame, by following the process explained in the process above, we need to compute the distance between the subspaces to perform classification. The natural metric for subspaces is the similarity, obtained from the canonical angles. Accordingly, in our framework, canonical angles are used as the distance measure between two shape subspaces.
The standard approach to measure the canonical angles between subspaces $\mathcal{Y}_1$ and $\mathcal{Y}_2$ is to calculate the singular values $\{\lambda_j\}_{j=1}^m$ of the correlation matrix between their basis matrices $\boldsymbol{Y}_1, \boldsymbol{Y}_2 \in \mathbb{R}^{d\times m}$, i.e. solving the SVD of $\boldsymbol{V}\boldsymbol{\Lambda}\boldsymbol{V}^\top = \boldsymbol{Y}_1^\top \boldsymbol{Y}_2$. This corresponds to finding the rotation of each basis that is closest to the opposing subspace. From solving this problem, the canonical angles can be obtained by $\theta_j = \cos^{-1}(\lambda_j),$ where $j = 1, \ldots, m$.

3.2.4 Grassmann Manifold

Now, we introduce here the concept of Grassmann manifold and how it is useful to correspond subspaces to vectors. The essence is to make a one-to-one mapping such that the similarities between subspaces is preserved, simplifying the representation and allowing general methods to be applicable.
Grassmann manifold $\mathcal{G}(m, d)$ is defined as the set of m-dimensional linear subspaces of $\mathbb{R}^d$. It is an $m(d-m)$-dimensional compact Riemannian manifold and can be derived as a quotient space of orthogonal groups $\mathcal{G}(m, d) = \mathcal{O}(d)/\mathcal{O}(m) \times \mathcal{O}(d-m)$, where $\mathcal{O}(m)$ is the group of $m \times m$ orthonormal matrices.
A Grassmann manifold can be embedded in a reproducing kernel Hilbert space by the use of a Grassmann kernel. In this case, the most popular kernel is the projection kernel k_p, which can be defined as $k_p(\mathcal{Y}_1, \mathcal{Y}_2) = \sum_{j=1}^m \cos^2\theta_j$, which is homologous to the subspace similarity. We can measure the distance between two points on a Grassmann manifold by using this projection kernel [?], and a subspace $\mathcal{Y}$ can be represented by a vector with regards to a reference subspace dictionary $\{\mathcal{Y}_q\}_{q=1}^N$ as $\boldsymbol{y} = k_p(\mathcal{Y}, \mathcal{Y}_q) = [k_p(\mathcal{Y}, \mathcal{Y}_1), k_p(\mathcal{Y}, \mathcal{Y}_2), \ldots, k_p(\mathcal{Y}, \mathcal{Y}_N)] \in \mathbb{R}^N$.

3.2.5 Grassmann Discriminant Analysis

We introduce a discriminatory mechanism to separate the classes of signals, which is the Grassmann discriminant analysis (GDA). Basically, GDA is conducted as kernel LDA with the Grassmann kernels. We first outline the algorithm of linear discriminant analysis (LDA) [?]. Let $\boldsymbol{x}_1, \ldots, \boldsymbol{x}_N$ be the data vectors and $y_1, \ldots, y_N$ ($y_i \in 1, \ldots, C$) be the class labels. Each class c has N_c number of samples. Let $\boldsymbol{\mu}_c = \frac{1}{N_c}\sum_{i|y_i=c} \boldsymbol{x}_i$ be the mean of class c, and $\boldsymbol{\mu} = \frac{1}{N}\sum_i \boldsymbol{x}_i$ be the overall mean. LDA searches for the discriminant direction $\boldsymbol{w}$ which maximizes the Rayleigh quotient $Ra(\boldsymbol{w}) = \boldsymbol{w}'\boldsymbol{S}_b\boldsymbol{w}/\boldsymbol{w}'\boldsymbol{S}_w\boldsymbol{w}$ where $\boldsymbol{S}_b$ and $\boldsymbol{S}_w$ are the between-class and within-class covariance matrices respectively:

$$\boldsymbol{S}_b = \frac{1}{N}\sum_{c=1}^{C} N_c(\boldsymbol{\mu}_c - \boldsymbol{\mu})(\boldsymbol{\mu}_c - \boldsymbol{\mu})^\top, \tag{3.1}$$

$$\boldsymbol{S}_w = \frac{1}{N}\sum_{c=1}^{C}\sum_{i|y_i=c} (\boldsymbol{x}_i - \boldsymbol{\mu}_c)(\boldsymbol{x}_i - \boldsymbol{\mu}_c)^\top. \tag{3.2}$$

The optimal $\boldsymbol{w}$ is obtained from the largest eigenvector of $\boldsymbol{S}_w^{-1}\boldsymbol{S}_b$. Since $\boldsymbol{S}_w^{-1}\boldsymbol{S}_b$ has rank $C-1$, there are $C-1$ optima $\boldsymbol{W} = [\boldsymbol{w}_1, \ldots, \boldsymbol{w}_{C-1}]$. By projecting data onto the space spanned by $\boldsymbol{W}$, we achieve dimensionality reduction and feature extraction of data onto the most discriminant subspace.
Kernel LDA [?, ?, ?] can be formulated by using the kernel trick as follows. Let $\Gamma : \mathbb{R}^d \to \mathcal{F}$ be a non-linear map from the input space $\mathbb{R}^d$ to a feature space $\mathcal{F}$, and $\Gamma = [\boldsymbol{\gamma}_1, \ldots, \boldsymbol{\gamma}_N]$ be the feature matrix of the mapped training points $\boldsymbol{\gamma}_i$. Assuming $\boldsymbol{w}$ is a linear combination of those feature vectors, $\boldsymbol{w} = \boldsymbol{\Gamma}\boldsymbol{\alpha}$, we can use the kernel trick and rewrite the Rayleigh quotient in terms of $\boldsymbol{\alpha}$ as:

$$\begin{aligned} Ra(\boldsymbol{\alpha}) &= \frac{\boldsymbol{\alpha}^\top\boldsymbol{\Gamma}^\top\boldsymbol{S}_b\boldsymbol{\Gamma}\boldsymbol{\alpha}}{\boldsymbol{\alpha}^\top\boldsymbol{\Gamma}^\top\boldsymbol{S}_w\boldsymbol{\Gamma}\boldsymbol{\alpha}} = \\ &= \frac{\boldsymbol{\alpha}^\top\boldsymbol{K}(\boldsymbol{V} - \boldsymbol{e}_N\boldsymbol{e}_N^\top/N)\boldsymbol{K}\boldsymbol{\alpha}}{\boldsymbol{\alpha}^\top(\boldsymbol{K}(\boldsymbol{I}_N - \boldsymbol{V})\boldsymbol{K} + \sigma^2\boldsymbol{I}_N)\boldsymbol{\alpha}} = \\ &= \frac{\boldsymbol{\alpha}^\top\boldsymbol{\Sigma}_b\boldsymbol{\alpha}}{\boldsymbol{\alpha}^\top(\boldsymbol{\Sigma}_w + \sigma^2\boldsymbol{I}_N)\boldsymbol{\alpha}}, \end{aligned} \tag{3.3}$$

where $\boldsymbol{K}$ is the kernel matrix, $\boldsymbol{e}_N$ is a vector of ones that has length N, $\boldsymbol{V}$ is a block-diagonal matrix whose c-th block is the matrix $\boldsymbol{e}_{N_c}\boldsymbol{e}_{N_c}^\top/N_c$, and $\boldsymbol{\Sigma}_b = \boldsymbol{K}(\boldsymbol{V} - \boldsymbol{e}_N\boldsymbol{e}_N^\top/N)\boldsymbol{K}$. For example, the kernel matrix, $\boldsymbol{K}$, is calculated as the similarity matrix between subspaces $\boldsymbol{Y}_q$ and $\boldsymbol{Y}_w$. The term $\sigma^2\boldsymbol{I}_N$ is used for regularizing the covariance matrix $\boldsymbol{\Sigma}_w = \boldsymbol{K}(\boldsymbol{I}_N - \boldsymbol{V})\boldsymbol{K}$. It is composed of the covariance shrinkage factor $\sigma^2 > 0$, and the identity matrix $\boldsymbol{I}_N$ of size N. The set of optimal vectors $\boldsymbol{\alpha}$ are computed from the eigenvectors of $(\boldsymbol{\Sigma}_w + \sigma^2\boldsymbol{I}_N)^{-1}\boldsymbol{\Sigma}_b$. We apply the GDA algorithm to the reference subspaces $\boldsymbol{Y}_i^c$ to generate reference vectors $\boldsymbol{y}_i^c$. When given an unknown bioacoustic signal $\boldsymbol{x}_{in}(t)$, we compute its SSA subspace $\mathcal{Y}_{in}$ and map it onto the manifold to generate a vector $\boldsymbol{y}_{in}$; then we predict its corresponding bioacoustic class (e.g. species) based on the nearest reference vector (1-NN).

Chapter 4

Proposed Method

Chapter 5

Experiments

In this chapter we conduct two experiments to demonstrate that our proposed method outperforms other traditional methods that have been introduced in previous chapters. The implementation is available at the website xxxx.

5.1 The Dataset

We collected data of 524 instances of a single-leg drop jump landing from 144 college football (soccer) players from the University of Tsukuba.

The dataset consists of the following attributes:

- 3 dimensional coordinates of 29 body markers capture by multiple infrared cameras.
- An integer (1 9) indicating the classification of ankle instability, labelled by an expert (label description: 1=Healthy, 2=Structural instability, 3=Subjective instability, 4=Sprained more than 3 times, 5=2 and 3, 6=2 and 4, 7=3 and 4, 8=2 and 3 and 4, 9=healthy but with a history of one or two sprains).
- Binary labels (0 or 1) indicating whether the single-leg drop jump was successful (0) or not (1). After consolation with an expert, we defined a successful jump as a jump where the subject was able to keep their balance on a single leg for more than 5 seconds after landing.
- Force plate data.
- Weight (kg) for each of the individual 144 athletes.

5.2 Evaluation Metrics

To evaluate the performance of different classification methods, we use a 5-fold cross-validation strategy to compute the classification accuracy, F1 score and the area under the receiver operating characteristic curve (AUC).

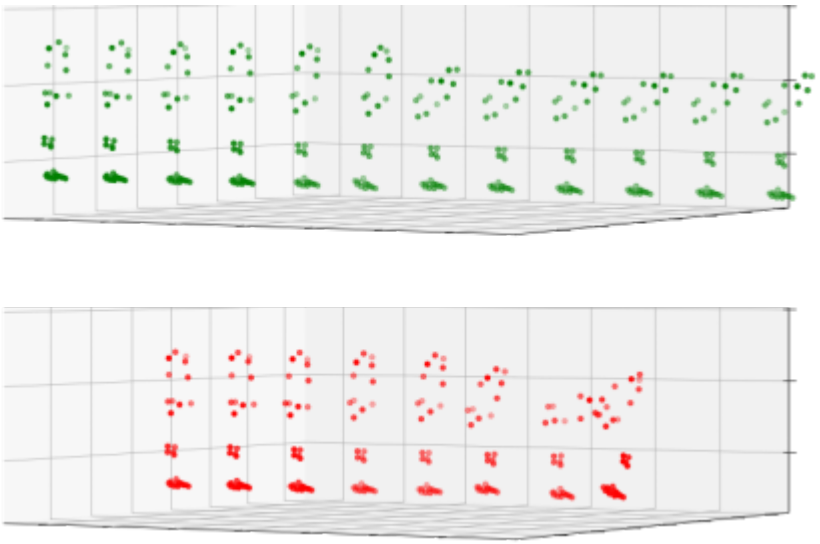

Figure 5.1: Two jump sequences sampled at 1fps. The successful jump is colored in green and the unsuccessful jump is colored in red.

Although accuracy is a sufficient metric for performance in datasets with symmetric classes distribution and class value, it is an inadequate metric for datasets with class imbalance and datasets where values of false positive and false negatives are differ.
Therefore, we included the two additional metrics explained above. These metrics are frequently used in medical cases such as cancer detection from images [10][11].

5.2.1 Accuracy

Accuracy is computed as the fraction of correct predictions.

$$\text{accuracy}(y, \hat{y}) = \frac{1}{n_{\text{samples}}} \sum_{i=0}^{n_{\text{samples}}-1} 1(\hat{y}_i = y_i)$$

5.2.2 F1 Score

The F1 score can be interpreted as an average of the classifier' s ability to:

- Not label as negative samples as a positive (i.e. Precision).
- Find all positive samples (i.e. Recall).

$$F_1 = 2 \times \frac{\text{precision} \times \text{recall}}{\text{precision} + \text{recall}}$$

5.2.3 Area Under the Curve

The receiver operating characteristic (ROC) plots the true positive rate (TPR) to the false positive rate (FPR) of a binary classifier with varying discrimination thresholds.
The area under the ROC curve (AUC) summarizes the information of the ROC in one number, between 0 and 1. AUC = 0.5 indicates an uniformative classifier (a classifier with uniform prediction for any sample) or random classifier if the classes are symmetric. Therefore no realistic classifiershould have an AUC < 0.5. AUC = 1 indicates a perfect classifier.
The algorithm to compute AUC with an in-depth explanation can be found in [12].

5.3 Experiment 1.

In this experiment we evaluate x classifiers accuracy on multiple binary classification problems regarding our single-leg drop jump dataset.

5.3.1 Experiment setup

We experiment with the following setup.

(A) Pose data up until landing.

(B) All pose data.

(C) Pose data + Force Plate data.

5.3.2 Results

5.3.3

Chapter 6

Discussion

Chapter 7

Conclusion

Appendices

Appendix A

Details regarding data

A.1 Details on the given data

A.2 Finding the time of landing

$$t = \sqrt{\frac{2h}{g}} = \sqrt{\frac{2 * 0.4441}{9.8}} \approx 0.39(s)$$

Therefore we find the frame where the average foot position on the y-axis is lowest, with the condition that the frame must be in within 39 frames after the highest point.

Index	Name
0	Cervical vertebra 7
1	Calcaneal tuberosity
2	Fibula Head
3	Greater trochanter
4	Suprasternal notch
5	Anterior superior iliac spine (L)
6	lateral epicondyle
7	medial malleolus
8	Posterior superior iliac spine (L)
9	medial condyle
10	medial epicondyle
11	lateral malleolus
12	Base of first metatarsal bone
13	Base of second metatarsal bone
14	Base of fifth metatarsal bone
15	Head of first metatarsal bone
16	Head of second metatarsal bone
17	Head of fifth metatarsal bone
18	Fibular trochlea of calcaneus
19	First distal phalanges
20	Anterior superior iliac spine (R)
21	Posterior superior iliac spine (L)
22	Acromion (L)
23	Acromion (R)
24	Sustentaculum tali
25	Thoracic vertebrae 8
26	Tibial tuberosity
27	Scaphoid bone
28	Xiphoid process

Acknowledgements

References

[1] Markus Stålbom, David Jonsson Holm, John B. Cronin, and Justin W.L. Keogh. Reliability of kinematics and kinetics associated with Horizontal Single leg drop jump assessment. A brief report. Journal of Sports Science and Medicine, Vol. 6, No. 2, pp. 261–264, 6 2007.

[2] Duncan P. Fransz, Arnold Huurnink, Idsart Kingma, and Jaap H. van Dieën. How does postural stability following a single leg drop jump landing task relate to postural stability during a single leg stance balance task? Journal of Biomechanics, Vol. 47, No. 12, pp. 3248–3253, 9 2014.

[3] Arnold Huurnink, Duncan P. Fransz, Idsart Kingma, Vosse A. de Boode, and Jaap H.van Dieën. The assessment of single-leg drop jump landing performance by means of ground reaction forces: A methodological study. Gait and Posture, Vol. 73, pp. 80–85, 9 2019.

[4] Duncan P. Fransz, Arnold Huurnink, Vosse A. De Boode, Idsart Kingma, and Jaap H. Van Dieën. Time to stabilization in single leg drop jump landings: An examination of calculation methods and assessment of differences in sample rate, filter settings and trial length on outcome values. Gait and Posture, Vol. 41, No. 1, pp. 63–69, 2015.

[5] ERIK A. WIKSTROM, MARK D. TILLMAN, and PAUL A. BORSA. Detection of Dynamic Stability Deficits in Subjects with Functional Ankle Instability. Medicine & Science in Sports & Exercise, Vol. 37, No. 2, pp. 169–175, 2 2005.

[6] Kyla A. Russell, Riann M. Palmieri, Steven M. Zinder, and Christopher D. Ingersoll. Sex differences in valgus knee angle during a single-leg drop jump. Journal of Athletic Training, Vol. 41, No. 2, pp. 166–171, 4 2006.

[7] WATANABE and S. Evaluation and Selection of Variables in Pattern Recognition. Computer and Information Science II, pp. 91–122, 1967.

[8] Taizo Iijima, Hiroshi Genchi, and Kenichi Mori. THEORY OF CHARACTER RECOGNITION BY PATTERN MATCHING METHOD. pp. 50–56, 1973.

[9] Akinari Sakai, Naoya Sogi, and Kazuhiro Fukui. Gait Recognition Based on Constrained Mutual Subspace Method with CNN Features. In 2019 16th International Conference on Machine Vision Applications (MVA), pp. 1–6. IEEE, 2019.

[10] Korsuk Sirinukunwattana, Shan E.Ahmed Raza, Yee Wah Tsang, David R.J. Snead, Ian A. Cree, and Nasir M. Rajpoot. Locality Sensitive Deep Learning for Detection and Classification of Nuclei in Routine Colon Cancer Histology Images. IEEE Transactions on Medical Imaging, Vol. 35, No. 5, pp. 1196–1206, 5 2016.

[11] Dan C. Cireşan, Alessandro Giusti, Luca M. Gambardella, JürgenSchmidhuber. Mitosis detection in breast cancer histology images with deep neural networks. In Lecture Notes in Computer Science (including subseries Lecture Notes in Artificial Intelligence and Lecture Notes in Bioinformatics), 第 8150 LNCS 巻, pp. 411–418, 2013.

[12] Tom Fawcett. An introduction to ROC analysis. Pattern Recognition Letters, 2006.